UNCERTAINTY EVALUATION OF THE 20 kN·m DEADWEIGHT TORQUE STANDARD MACHINE

Koji Ohgushi[1], Takashi Ota[1] and Kazunaga Ueda[1]

[1]Mass and Force Standard Section, NMIJ/AIST, Japan

ABSTRACT

A deadweight-type torque standard machine of 20 kN·m rated capacity (20 kN·m-DWTSM) has been designed and developed by the National Metrology Institute of Japan (NMIJ) at the National Institute of Advanced Industrial Science and Technology (AIST). Each uncertainty contribution comes mainly from the performance of each mechanical part of the 20 kN·m-DWTSM. Authors evaluated the uncertainty of the mass of the linkage weights, local acceleration of gravity, influence of air buoyancy on deadweight loading, initial moment-arm length (including CMM measurement and temperature compensation), and sensitivity of the fulcrum. This report deals especially with evaluation of the remaining contributions, namely the influence of arm flexure and reference line variation at the end of the moment-arm on best measurement capability (BMC). Estimation of BMC in the 20 kN·m-DWTSM gave a relative expanded uncertainty of less than 7.0×10^{-5} ($k = 2$) for the calibration range from 200 N·m to 20 kN·m.

1. INTRODUCTION

To meet the demands of the national torque standard for Japanese industry, the torque range realized with torque standard machines at the NMIJ/AIST is being expanded. The uncertainty of deadweight-type torque standard machine of 1 kN·m rated capacity (1 kN·m-DWTSM) has already been evaluated, and the machine has been provided for calibration service (calibration range: 5 N·m - 1 kN·m, relative expanded uncertainty $U_{\mathrm{tsm\_01}} = 4.9 \times 10^{-5}$ ($k = 2$))[1].

The authors have developed another deadweight-type torque standard machine of 20 kN·m rated capacity (20 kN·m-DWTSM). Uncertainty evaluation and dissemination of standard are also expected for the establishment of the torque traceability system in this relatively high capacity torque range, which is destined for use in the field of large torque wrenches, marine engines, large generators, and so on.

The uncertainty of the torque realized by the torque standard machine is estimated from the composition of each uncertainty contribution in the assembled structural parts. This report describes uncertainty evaluation results, in particular the influence of arm flexure and reference line variation at the ends of the moment-arm on best measurement capability (BMC).

2. SUMMARY OF EVALUATED UNCERTAINTY CONTRIBUTIONS

The uncertainties have already been evaluated for mass of linkage weights, local acceleration of gravity, influence of air buoyancy on the force generated by deadweight loading, initial moment-arm length (including CMM measurement and temperature compensation), and sensitivity error and sensitivity reciprocal of the fulcrum. Brief explanations are as follows.

2.1. MASS OF LINKAGE WEIGHTS

An uncertainty u_{mass} of less than 3.5×10^{-6} was obtained for the mass of linkage weights as a relative standard uncertainty by the NMIJ calibration, which is traceable to the national mass

standard[2].

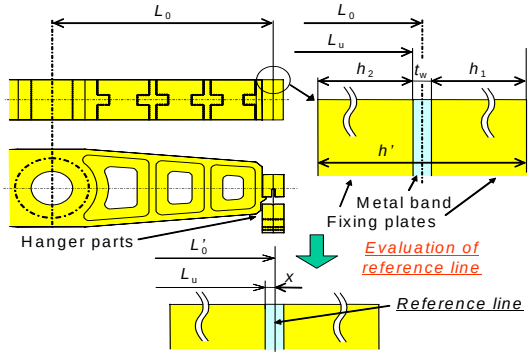

Figure 1: Structure of the moment-arm

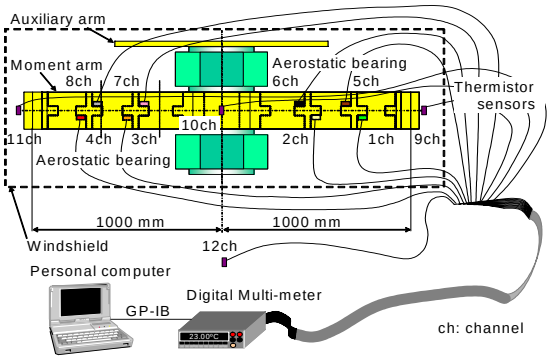

Figure 2: Temperature measurement system

2.2. ACCELERATION OF GRAVITY

The local acceleration of gravity at the place of the 20 kN·m-DWTSM was measured by the FG5 absolute gravimeter at NMIJ. The measurement value g_{local} was 9.7994841 m/s^2. A relative standard uncertainty u_{grav} of 6.3 × 10^{-7} was obtained, including the influence of tide and altitude.

2.3. INFLUENCE OF AIR BUOYANCY

The influence of air buoyancy on the force realized by the deadweights was evaluated by controlling room temperature and humidity and observing the atmospheric pressure. A relative standard uncertainty u_{buoy} of less than 5 × 10^{-6} was obtained within the variation of ruled ambient conditions (23 °C ± 1 °C, 30-60 %RH and 986-1040 hPa).

2.4. INITIAL MOMENT-ARM LENGTH

A coordinate measurement machine (CMM) was used to measure the initial moment-arm length under a temperature environment of 23 °C[2]. Figure 1 is a schematic diagram of the moment-arm. The results of the initial length measurement were as follows:

$L_{u(L)}$ = 999.8109 ± 0.0019 mm, $L_{u(R)}$ = 999.8421 ± 0.0019 mm,
$t_{w(L)}$ = 0.4053 ± 0.0033 mm, $t_{w(R)}$ = 0.4061 ± 0.0033 mm,
$L_{0(L)}$ = 1000.0153 ± 0.0038 mm and $L_{0(R)}$ = 1000.0452 ± 0.0038 mm.

(R) is the arm length on the right side and (L) the left side. The latter values after ± were standard uncertainties. The relative standard uncertainty of initial arm length measurement (CMM measurement) was 3.8 × 10^{-6}.

To allow for temperature compensation of arm length (which was made of austenitic stainless steel), the temperature of the moment-arm was measured during torque calibration conditions, as shown in Figure 2[3]. Figure 3 shows an example of the measurement results over about eight hours. It was found that estimation of the arm temperature (1ch-8ch) was possible by monitoring the temperatures of two thermometers (9ch and 11ch), put on adjacent to both the ends of the arm. The relative combined standard uncertainty of the arm length u_{act_lgt}, including CMM measurement and length variation due to temperature change, was less than 7.5 × 10^{-6}.

2.5. SENSITIVITY OF THE FULCRUM

The double aerostatic bearings are built in the form of a fulcrum. Sensitivity of the fulcrum was verified by an arm-balancing test in which the torque transducer was not installed. Weights of equal mass were loaded at both tips of the moment-arm, and the inclined level was measured with linear scales (photo-electric reflection type, resolution 0.2 μm) put on each end of the auxiliary arm with the loading and unloading of small weights. A sensitivity reproducibility u_{ssv} of 4.6 × 10^{-7} and a sensitivity reciprocal u_{sr} of 5.0 × 10^{-6} were obtained as relative standard uncertainties[3].

3. EVALUATION OF REMAINING UNCERTAINTY CONTRIBUTIONS

The influence of arm flexure and reference line variation at the end of the moment-arm on BMC had not been reported previously. The experimental procedures and results for these evaluations are described as follows.

3.1. INFLUENCE OF ARM FLEXURE

The arm length variation due to arm flexure caused by the deadweight loading was examined. Figure 4 shows the interferometer system used to measure arm length variation (He-Ne laser, wavelength 633 nm, resolution 0.01 μm).

The measurement results are shown in Figure 5(a) for the left-sided (counterclockwise) variation $\Delta L_{0(L)}$, and in Figure 5(b) for the right-sided (clockwise) variation $\Delta L_{0(R)}$ when the torque was loaded in each direction over the whole range of the 20 kN·m-DWTSM. The arm length variations became asymmetric because small working and assembling errors in the arm parts could affect the deformation. The quantities of variation were, however, quite small. The standard relative uncertainty of the influence of the arm-flexure $u_{\mathrm{flx\_lgt}}$ was within 2.0×10^{-6}, provided that the maximum variation was half the width of the rectangular distribution (Type B).

3.2. INFLUENCE OF REFERENCE LINE VARIATION

To evaluate the arm length more correctly, the possibility of the variation in the loading point (called "reference line") with deadweight loading should be considered[1]. Metal bands (MBs) are used for the loading points as shown in Figure 1. Here the arm length is redefined according to the lower diagram in Figure 1 and the following equations:

$$L_{0(\mathrm{R})}' = L_{\mathrm{u}(\mathrm{R})} + x_{(\mathrm{R})}\,, \qquad L_{0(\mathrm{L})}' = L_{\mathrm{u}(\mathrm{L})} + x_{(\mathrm{L})}\,. \tag{1}$$

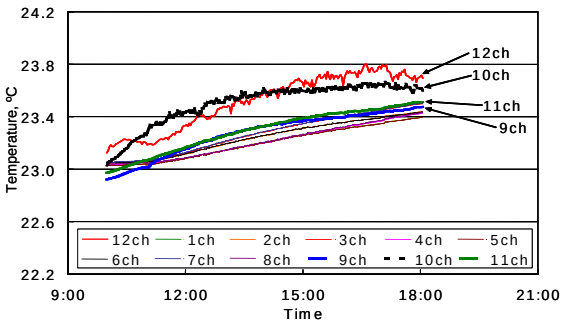

Figure 3: Temperature measurement results

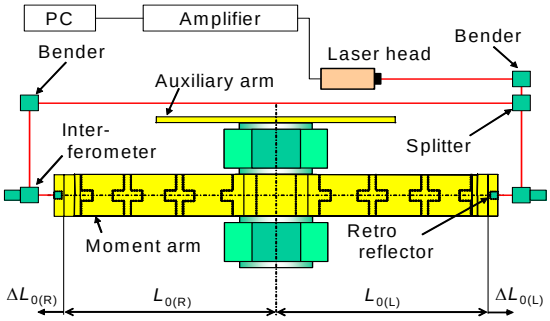

Figure 4: Apparatus used to measure arm length variation

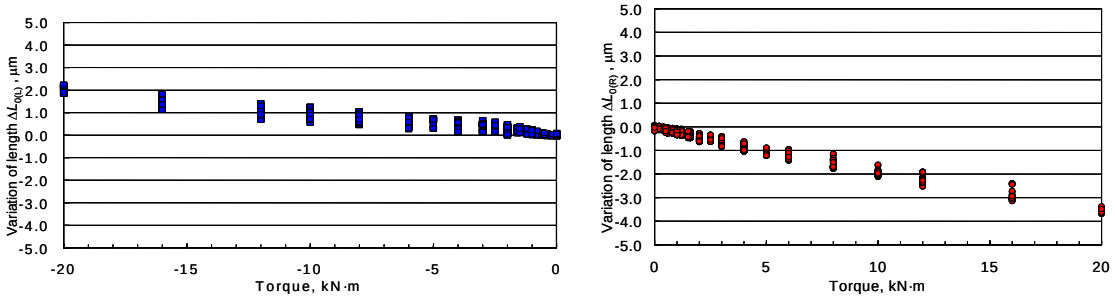

(a): Left side **(b):** Right side

Figure 5: Results of measurement of length variation due to arm flexure

3.2.1. ASYMMETRIC STRESS DISTRIBUTION MODEL

Reference line variation may be attributable to the asymmetric stress distribution in the thickness direction of the MBs. It was presumed that the asymmetric distribution was caused by

the outward bend of the MBs. This drives the reference line inward, i.e., makes the effective arm length shorter than that in the case where there is no bend (i.e. the arm length measured by the CMM).

To verify this effect, another arm-balancing test was conducted changing the MB thickness from 400 μm to 200 μm. Weights of equal mass were loaded at each end of the moment-arm. Small torque ratio between clockwise and counterclockwise torques was measured by using the torque transducers of small rated capacity. Although this test gives only the relative value of arm length between right and left sides and the difference in the location of the reference lines at 400 μm and 200 μm MB thickness, the test can make the location range of the reference line narrower than the MB thickness. This means that the uncertainty of arm length can be predicted more correctly.

In eq. (1), it is assumed that $x_{(R)} > x_{(L)}$ from the results of length measurement with the CMM. The arm-balancing tests in four patterns were conducted while changing the MB thickness at each side, as shown in Table 1. The symbols for relative positions are defined in Figure 6(a) and 6(b). The relationship between reference line position and torque ratio given by the arm-balancing test is expressed as:

$$\frac{\Delta T}{T} = \frac{(L_{u(R)} + x_{(R)}) \cdot W - (L_{u(L)} + x_{(L)}) \cdot W}{L \cdot W} = C_A' + \frac{x_{(R)} - x_{(L)}}{L}, \tag{2}$$

where W is the force generated by deadweight loading, L is the nominal arm length, and

$$C_A' = \frac{L_{u(R)} - L_{u(L)}}{L}. \tag{3}$$

Each relative position in Table 1 is obtained by the experiments from A to D as follows:

Table 1: Conditions used in the arm-balancing tests

Experiment	MB thickness (L), μm	MB thickness (R), μm	Relative position
A	400	400	$\delta x_{RL}\|_{400} = x_{(R)}\|_{400} - x_{(L)}\|_{400}$
B	400	200	$\delta x_{RL}\|_{200\text{-}400} = x_{(R)}\|_{200} - x_{(L)}\|_{400}$
C	200	400	$\delta x_{RL}\|_{400\text{-}200} = x_{(R)}\|_{400} - x_{(L)}\|_{200}$
D	200	200	$\delta x_{RL}\|_{200} = x_{(R)}\|_{200} - x_{(L)}\|_{200}$

$\Rightarrow$ $\delta x_{(R)}|_{400\text{-}200} = x_{(R)}|_{400} - x_{(R)}|_{200}$, $\delta x_{(L)}|_{400\text{-}200} = x_{(L)}|_{400} - x_{(L)}|_{200}$

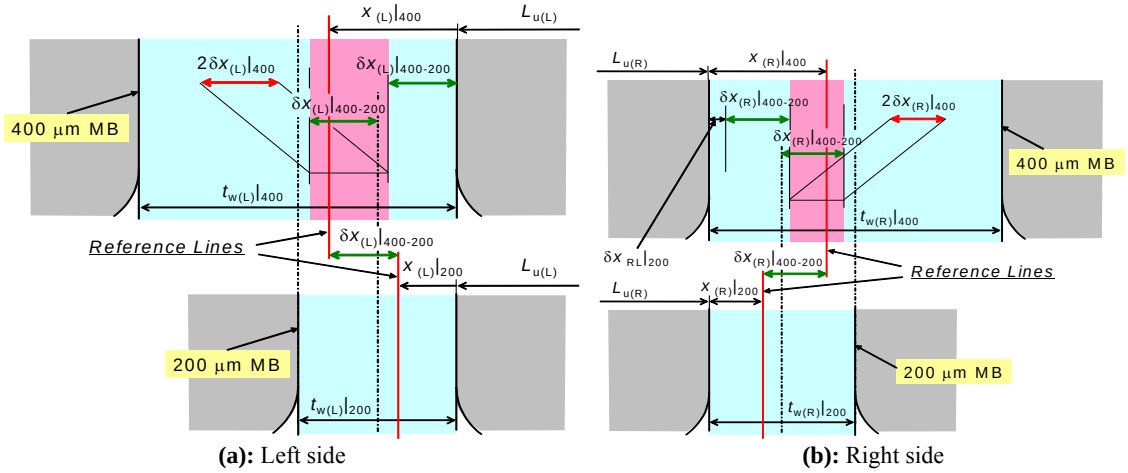

(a): Left side **(b):** Right side

Figure 6: Definitions of reference line positions

$$\left.\frac{\Delta T}{T}\right|_A = C_A' + \frac{x_{(R)}\big|_{400} - x_{(L)}\big|_{400}}{L} = C_A' + \frac{\delta x_{RL}\big|_{400}}{L} \tag{4a}$$

$$\left.\frac{\Delta T}{T}\right|_{\mathrm{B}} = C_{\mathrm{A}}' + \frac{x_{(\mathrm{R})}|_{200} - x_{(\mathrm{L})}|_{400}}{L} = C_{\mathrm{A}}' + \frac{\delta x_{\mathrm{RL}}|_{200-400}}{L} \tag{4b}$$

$$\left.\frac{\Delta T}{T}\right|_{\mathrm{C}} = C_{\mathrm{A}}' + \frac{x_{(\mathrm{R})}|_{400} - x_{(\mathrm{L})}|_{200}}{L} = C_{\mathrm{A}}' + \frac{\delta x_{\mathrm{RL}}|_{400-200}}{L} \tag{4c}$$

$$\left.\frac{\Delta T}{T}\right|_{\mathrm{D}} = C_{\mathrm{A}}' + \frac{x_{(\mathrm{R})}|_{200} - x_{(\mathrm{L})}|_{200}}{L} = C_{\mathrm{A}}' + \frac{\delta x_{\mathrm{RL}}|_{200}}{L} \tag{4d}$$

The reference line positions and their location ranges are estimated by the following procedure:

(a) From the assumption that $x_{(\mathrm{R})} > x_{(\mathrm{L})}$, $\delta x_{\mathrm{RL}}|_{200}$ should be a positive value. Then the lower limit of the reference line position for the 400 μm MB on the right side can be determined as the sum of $\delta x_{\mathrm{RL}}|_{200}$ and $\delta x_{(\mathrm{R})}|_{400\text{-}200}$.

(b) The upper limit can be expressed as the sum of $(t_{\mathrm{w(R)}}|_{200})/2$ and $\delta x_{(\mathrm{R})}|_{400\text{-}200}$, because $x_{(\mathrm{R})}|_{200} \leq (t_{\mathrm{w(R)}}|_{200})/2$ is true from the hypothesis of the inwardly biased stress distribution.

(c) Therefore, the shaded range in Figure 6(b) corresponds to the possible width of the reference line on the right side. Provided that this range is the whole width of the rectangular distribution $2\delta x_{(\mathrm{R})}|_{400}$, then the median value is simply the position of the reference line, i.e.:

$$\delta x_{(\mathrm{R})}|_{400} = (t_{\mathrm{w(R)}}|_{200})/4 - (\delta x_{\mathrm{RL}}|_{200})/2\,, \tag{5}$$

$$x_{(\mathrm{R})}|_{400} = \delta x_{\mathrm{RL}}|_{200} + \delta x_{(\mathrm{R})}|_{400-200} + \delta x_{(\mathrm{R})}|_{400}\,. \tag{6}$$

(d) On the other hand, the lower limit of the reference line position for the 400 μm MB on the left side can be easily determined as $\delta x_{(\mathrm{L})}|_{400\text{-}200}$ itself.

(e) The upper limit can also be expressed as the sum of $(t_{\mathrm{w(L)}}|_{200})/2$ and $\delta x_{(\mathrm{L})}|_{400\text{-}200}$ because $x_{(\mathrm{L})}|_{200} \leq (t_{\mathrm{w(L)}}|_{200})/2$ is true from the hypothesis of inwardly biased stress distribution.

(f) Therefore, the shaded range in Figure 6(a) corresponds to the possible width of the reference line on the left side. Provided that this range is the whole width of the rectangular distribution $2\delta x_{(\mathrm{L})}|_{400}$, then $\delta x_{(\mathrm{L})}|_{400}$ can be simply expressed as:

$$\delta x_{(\mathrm{L})}|_{400} = (t_{\mathrm{w(L)}}|_{200})/4\,. \tag{7}$$

(g) $x_{(\mathrm{L})}|_{400}$ can be calculated from eq. (2) and eq. (6).

3.2.2. EXPERIMENTAL PROCEDURE

The arm-balancing test was conducted using deadweight series of 200 N × 10 disks, 500 N × 10 disks and 1 kN × 10 disks, with equivalent torque steps of 0.2, 0.4, 1 and 2 kN·m, 0.5, 1, 2.5 and 5 kN·m, and 1, 2, 4, 6, 8 and 10 kN·m, respectively. These loadings were repeated three times for each of the conditions A, B, C, and D. The torque ratio was recorded from the output of the torque transducers of 200 N·m rated capacity (for 200 N deadweight series) and 1 k N·m rated capacity (for 500 N and 1 kN dead weight series).

3.2.3. EXPERIMENTAL RESULTS

Figure 7 shows the measured torque ratio obtained by experiments A to D in Table 1. It is obvious that the torque ratios were almost constant under the same conditions. The maximum deviation (in experiment A) was 1.3×10^{-5}. From the values at T = 10 kN·m, then, the re-estimated values of arm length at 23 °C when using a 400 μm MB on each side were calculated as follows:

$x_{(\mathrm{L})} = x_{(\mathrm{L})}|_{400} = 0.1458 \pm 0.0304$ mm, $x_{(\mathrm{R})} = x_{(\mathrm{R})}|_{400} = 0.1583 \pm 0.0270$ mm,
$L_{0(\mathrm{L})}' = 999.9567 \pm 0.0312$ mm and $L_{0(\mathrm{R})}' = 1000.0004 \pm 0.0279$ mm.

The latter values show standard uncertainties. The measurement and calculation results are indicated in Table 2 for each length defined in Figure 6, together with the related uncertainties. The measurement results for the MB thicknesses themselves are also shown in Table 2. The

uncertainty

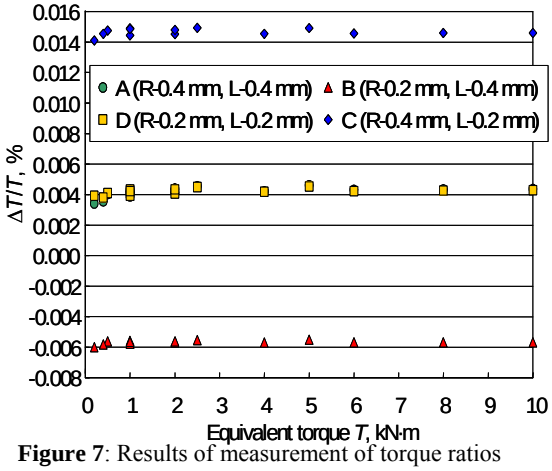

Figure 7: Results of measurement of torque ratios

Table 2: Each Length of MB and related uncertainties

Lengths			
$t_{w(L)\|400}$, μm	405.3	$t_{w(R)\|400}$, μm	406.1
$t_{w(L)\|200}$, μm	204.0	$t_{w(R)\|200}$, μm	202.7
		$\delta x_{RL\|200}$, μm	11.6
$\delta x_{(L)\|400\text{-}200}$, μm	101.0	$\delta x_{(R)\|400\text{-}200}$, μm	101.8
$\delta x_{(L)\|400}$, μm	51.0	$\delta x_{(R)\|400}$, μm	44.9
$x_{(L)\|400}$, μm	145.8	$x_{(R)\|400}$, μm	158.3
Uncertainty			
$u(t_{w(L)\|200})$, μm	1.4	$u(t_{w(R)\|200})$, μm	1.4
$u(\delta x_{(L)\|400\text{-}200})$, μm	6.8	$u(\delta x_{(R)\|400\text{-}200})$, μm	6.8
$u(\delta x_{(L)\|400})$, μm	29.6	$u(\delta x_{(R)\|400})$, μm	26.1
$u(x_{(L)\|400})$, μm	30.4	$u(x_{(R)\|400})$, μm	27.0
$U(x_{(L)\|400})$, $\times 10^{-6}$	60.9	$U(x_{(R)\|400})$, $\times 10^{-6}$	54.0
$U_{load.dpd}$, $\times 10^{-6}$			12.9
$U_{tra.res}$, $\times 10^{-6}$			5.4
$U_{load.lgt(L)}$, $\times 10^{-6}$	62.4	$U_{load.lgt(R)}$, $\times 10^{-6}$	55.8

ascribable to the deadweight load dependency of the arm lengths (reference line movement) is expressed by $U_{load.lgt}$, combining the net torque deviations due to load dependency ($U_{load.dpd} = 1.3 \times 10^{-5}$), the uncertainty of reference line position of the MB ($U(x|_{400})$), and the resolution of the torque transducers ($U_{tra.res}$). Here the coverage factors were all $k = 2$.

4. CONCLUSION

The relative expanded uncertainty of the realized torque in the 20 kN·m-DWTSM could be calculated by the following equation:

$$U_{tsm\_20} = k \cdot \sqrt{u_{mass}^2 + u_{grav}^2 + u_{buoy}^2 + u_{act.lgt}^2 + u_{flx.lgt}^2 + u_{load.lgt}^2 + u_{ssv}^2 + u_{sr}^2} \,. \qquad (8)$$

Then, $U_{tsm\_20} = 6.6 \times 10^{-5}$ ($k = 2$) were obtained. The BMC, which equals the relative expanded uncertainty of the calibration with an almost ideal torque transducer, could be achievable less than 7.0×10^{-5} for the calibration range from 200 N·m to 20 kN·m. Some bilateral comparisons between other national metrology institutes and NMIJ have been conducted over this torque range. The results will be reported on the next occasion.

REFERENCES

[1] K. Ohgushi, T. Ota and K. Ueda, "Load Dependency of The Moment-arm Length in The Torque Standard Machine", Proceedings of XVII IMEKO World Congress, Dubrovnik/Croatia, 2003, **3**, pp. 383-388.

[2] K. Ohgushi, T. Ota, K. Ueda and E. Furuta, "Design and Development of The 20 kN·m Deadweight Torque Standard Machine", *VDI-Berichte*, **1685**, 2002, pp. 327-332.

[3] K. Ohgushi, T. Ota and K. Ueda, "Uncertainty Evaluation of the 20 kN·m Torque Standard Machine - 1st Report - Temperature Compensation of the Arm Length and Sensitivity Evaluation of the Fulcrum – (in Japanese)", Proceedings of the 20th Sensing Forum, Tokyo/Japan, 2003,
pp. 233-237.

Addresses of the Authors:

Koji Ohgushi, Takashi Ota and Kazunaga Ueda, Mass and Force Standard Section, National Metrology Institute of Japan/AIST, Tsukuba Central 3, 1-1-1 Umezono, Tsukuba, 305-8563, Japan. k.ohgushi@aist.go.jp